Optics and Spectroscopy, 2024, Vol. 132, No. 8

02

Optical spectroscopy of inorganic lead halide perovskite $CsPbBr_3$ single crystals

© *V.E. Anikeeva*[1,2], *N.Yu. Boldyrev*[1], *O.I. Semenova*[3], *K.N. Boldyrev*[1], *M.N. Popova*[1]

[1] Institute of Spectroscopy, Russian Academy of Sciences, Troitsk, Moscow, Russia
[2] National Research University Higher School of Economics, Moscow, Russia
[3] Rzhanov Institute of Semiconductor Physics, Siberian Branch, Russian Academy of Sciences, Novosibirsk, Russia

E-mail: vanikeeva@hse.ru

Received June 28, 2024
Revised June 28, 2024
Accepted July 29, 2024

The paper presents the results of the temperature dependences study of the luminescence spectra (3.6−120 K) upon excitation by 405 nm light and of the non-contact measured photoconductivity spectra (3.6−300 K) of a $CsPbBr_3$ single crystal. In the low-temperature photoluminescence (PL) spectrum, in addition to the self-trapped exciton line (2.318 eV at 10 K), a rich structure, possibly related to exciton-impurity complexes, and a broad band with a maximum at about 2.24 eV, which may be the PL of impurity or defect centers, are observed. The photoconductivity (PC) spectrum contains two narrow peaks at the frequencies of intense excitonic PL lines and a wide continuum corresponding to band-to-band absorption. While PL quenches with increasing temperature, PC signal increases. Based on the analysis of the temperature dependences of the integral intensities of the exciton peak in the PL and PC, the activation energies of 12 ± 3 and 77 ± 10 meV were found for the processes leading to the decay of the self-trapped exciton, accompanied by the quenching of PL and the appearance of charge carriers. An estimate of the exciton binding energy in a $CsPbBr_3$ single crystal was obtained: $E_b = 65 \pm 13$ meV.

Keywords: perovskites, $CsPbBr_3$ single crystal, optical spectroscopy, excitons, photoluminescence, photoconductivity.

DOI: 10.61011/EOS.2024.08.60022.6833-24

Introduction

Lead-halide perovskites ABX_3 (where Cs^+ or the organic cations $CH_3NH_3^+$ (MA), $CH(NH_2)_2^+$ (FA) may serve as the A cation, the Pb^+ cation may serve as the B cation, the I^-, Br^- or Cl^- halogen anions may serve as the X anions) are promising materials for applications in photovoltaic devices and electromagnetic radiation generating devices [1–4]. These materials have a wide scope of application due to their optoelectronic properties, i.e. low density of traps, high quantum yield of luminescence, band gap most suitable for solar radiation, high diffusion length of charge carriers [1–3]. In particular, the all-inorganic perovskite compound $CsPbBr_3$ has a better thermal stability compared with hybrid organic-inorganic alternatives $MAPbBr_3$ and $FAPbBr_3$. Numerous research teams make efforts to improve the properties of photovoltaic and light emitting devices based on cesium-halide-perovskites through the advancement of thin film, doping and micro/nanocrystal technologies, including those embedded in various semiconductor matrices, and layered structure technologies [3,5–12]. Study of single crystals is of paramount importance for understanding physical processes in cesium-halide perovskites.

This is the first study that investigates photoluminescence (PL) and photoconductivity (PC) spectra of $CsPbBr_3$ on the same single crystal in a wide temperature range (3.6−300 K) with the spectral resolution up to 0.25 meV. Temperature dependences of integrated exciton peak intensities in PL and PC were examined, activation energies of processes inducing dissociation of an autolocalized exciton, exciton PL quenching and formation of charge carriers were found.

The authors dedicate this work to the memory of Vladimir M. Agranovich — an outstanding scientist and colleague at the Institute of Spectroscopy RAS. V.M. Agranovich was interested in hybrid organic-inorganic materials for a long time. He elaborated the theory of Frenkel-Vanier-Mott hybrid excitons that occur in nanostructures containing organic and semiconductor quantum wells [13], took a keen interest in studies of new promising photovoltaic materials — hybrid organic-inorganic halide perovskites ABX_3 ($X^- = I^-$, Br^-, Cl^-, $B^{2+} = Pb^{2+}$, Sn^{2+}, $A^+ = MA^+$, FA^+) that were carried out by his students [14]. Besides organic cations, the perovskite structure of halide compounds is stabilized only by one inorganic cation Cs^+. Therefore, all-inorganic cesium halide perovskites are on a par with hybrid halide perovskites.

Experiment

A. Synthesis of $CsPbBr_3$ single crystals

A traditional method for growing crystals from a saturated solution with slow precision decrease in the solution tem-

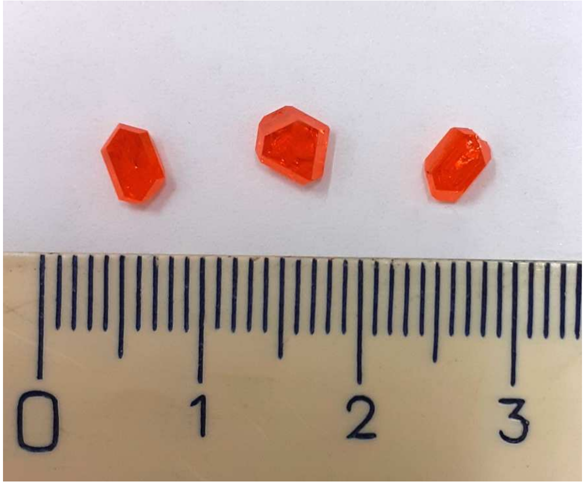

Figure 1. $CsPbBr_3$ single crystals.

perature was used. An aqueous hydrobromic acid solution (HBr 48%) was used as a solvent. A saturated solution was prepared using the solubility curve data of $CsPbBr_3$ in the HBr aqueous solution taken from [15]. The starting salts (lead bromide ($PbBr_2$) and cesium bromide (CsBr), ACS grade) were mixed in 1:1 equimolar ratio. For this, accurately weighed 1.9078 g $PbBr_2$ and 1.1071 g CsBr were mixed and dissolved in 50 ml HBr. The solution was heated on a water bath to 80°C and the saturated solution was placed into a reactor for crystal growing. A fine seed single crystal was also placed into the reactor. Then controlled solution temperature decrease to room temperature was performed at a rate of 0.15 deg/h. Then the crystals were removed from the solution, rinsed in ether and dried. The prepared orange single crystals had natural faces and good optical quality (Figure 1).

X-ray diffraction analysis for the synthesized samples was conducted using a procedure similar to that described in [16]. It has been shown previously in [17] that at $T \sim 300$ K the symmetry was monoclinic, rather than orthorhombic, and a second-order phase transition with space group change $Pm - P21/m$ took place at the same temperature. Similar changes are also observed in the prepared single crystal, i.e. at $T \sim 300$ K there are superlattice reflections considering which the cell parameters are as follows: $a = 11.6338(13)$, $b = 11.7125(12)$, $c = 11.6625(11)$ Å, $\beta = 89.65(1)^\circ$, space group is $P21/m$.

B. Measurement of transmission and PL spectra

Transmission spectra shown in this work were measured in the range of 8000−20000 cm^{-1} (1.0−2.5 eV) covering the fundamental absorption region of $CsPbBr_3$. PL was excited by the $\lambda = 405$ nm diode laser and recorded in the spectral region of 625−500 nm (2.0−2.5 eV). Spectra were recorded using the Bruker IFS 125HR high-resolution Fourier spectrometer with Si detector. Spectral resolution (up to 2 cm^{-1}) was selected such that to avoid spectrum distortions. Temperature dependences of spectra in the range from 3.6 K to 320 K were examined using the Sumitomo SRP-082 closed-cycle cryostat. A 1.4 mm thick $CsPbBr_3$ single crystal was fixed on a copper substrate using silver paste. Then the substrate was attached to the cryostat's copper finger in such a way that the natural (100) face of the crystal was oriented perpendicularly to the incident radiation.

B. Noncontact photoconductivity measurement

PC spectra of the $CsPbBr_3$ crystal were measured using the noncontact photoconductivity (NCPC) method. The crystal was placed between the capacitor plates. One of the plates was semi-transparent (metal mesh), the cryostat's copper finger served as the second plate. Capacitor with the sample placed into the cryostat was connected to a circuit with an electromagnetic coil, which created an oscillatory circuit. The coil and capacitor were selected to ensure the oscillatory circuit resonance frequency of ~ 180 MHz. Halogen lamp light modulated by the Fourier spectrometer was incident normally onto the sample through the semi-transparent plate. When the electrical characteristics of the sample changed by exposure to light (carrier generation), a resonance frequency shift occured due to a change in the capacitor capacitance. Frequency shift signal was applied to the Fourier spectrometer input channel and, thus, PC spectrum was recorded.

Results

Figure 2 shows the temperature-dependent PL spectra. PL is very weak above 110 K, two asymmetric peaks are observed in the range of 110−40 K, new features occur below 40 K and are enhanced as the temperature decreases further, lines alternate in intensity (Figure 2, *a, b*). At low temperatures (3.6−15 K), there are two intense narrow lines with an intermediate structure between them. Positions of peaks of this structure are shown in Figure 2, *c*. A broad band is observed on the long-wavelength side. Decomposition of the spectrum into components gives 2.24 eV for the position of the maximum of the broad band at 3.6 K. Figure 2, *d* shows comparison of the PL spectra at the lowest (3.6 K) and highest (320 K) temperatures studied. In the place of two narrow lines observed at a low temperature, a broad asymmetric band appears at a high temperature. There is another broad low-intensity peak on the low-frequency side.

Figure 3 shows PC spectra. It can be seen that the spectrum at room temperature exhibits one peak with a shoulder in the long-wavelength region and a long „tail“ towards the short-wavelength side. As the temperature decreases to approx. 200 K, the peak splits and as many

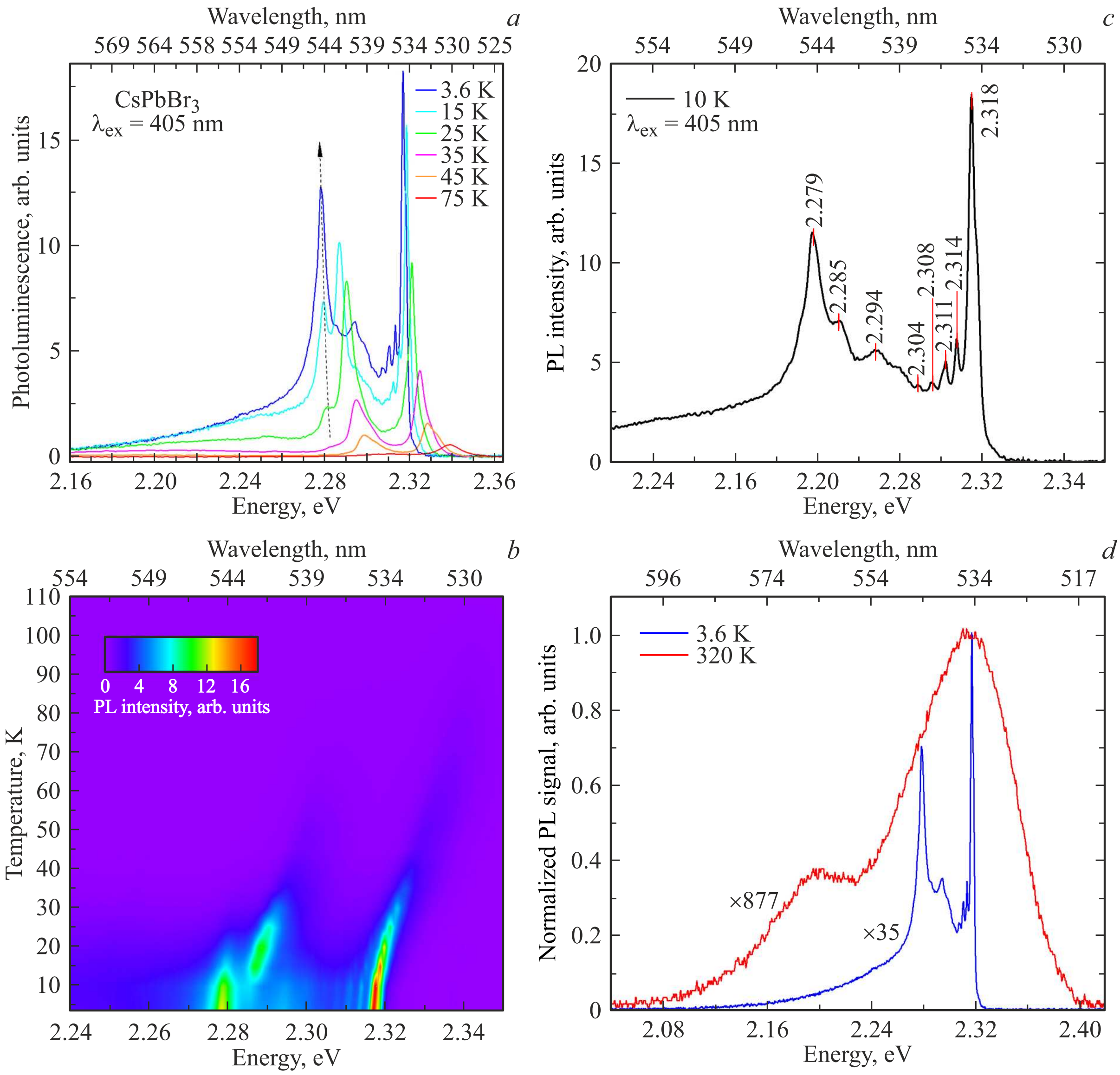

Figure 2. PL spectra of the $CsPbBr_3$ single crystal (*a*) at several temperatures, (*b*) in the form of an intensity map, (*c*) at 10 K indicating the frequencies of spectral features, (*d*) at 320 K and 3.6 K, normalized for comparison. The excitation wavelength is $\lambda_{ex} = 405$ nm.

as three peaks are observed at 150 K, and at temperatures below 70 K the spectrum starts to decrease in intensity and almost disappears at 5 K.

Discussion

In [18–20], reflection spectra of the $CsPbBr_3$ single crystals displayed a strong exciton-polariton resonance at 2.322 eV at 10 K and an exciton luminescence peak shifted by 4−10 meV into the long-wavelength side (2.318 eV). In the above-mentioned studies, the exciton luminescence line had a symmetric form with a small shoulder on the low-frequency side. However, an intense line shifted by ~ 38 meV towards the long-wavelength region, intermediate structure and broad long-wavelength band (as in our case) were not observed. It is supposed that an intense PL line 2.318 eV in our spectra that was also observed in [18–20] corresponds to an autolocalized exciton, while lower-frequency lines are induced by transitions in the exciton-impurity complexes. If these lines were photonic repetitions of the exciton line [21] or resulted from the Rashba effect [22–24], they would be observed in all crystals. Studies [18–20] most likely investigated more perfect crystals than those used in this work and in [21–24]. A broad long-wavelength band that was also observed in [21,22,25,26] may result from PL of uncontrolled impurities or defects. Investigation of their nature is not in the scope of this work.

As the temperature increases, the exciton luminescence shifts into a short-wavelength side (Figure 2, *a*, *b*) and then back into the long-wavelength side (a detailed temperature dependence was not recorded due to a very low PL

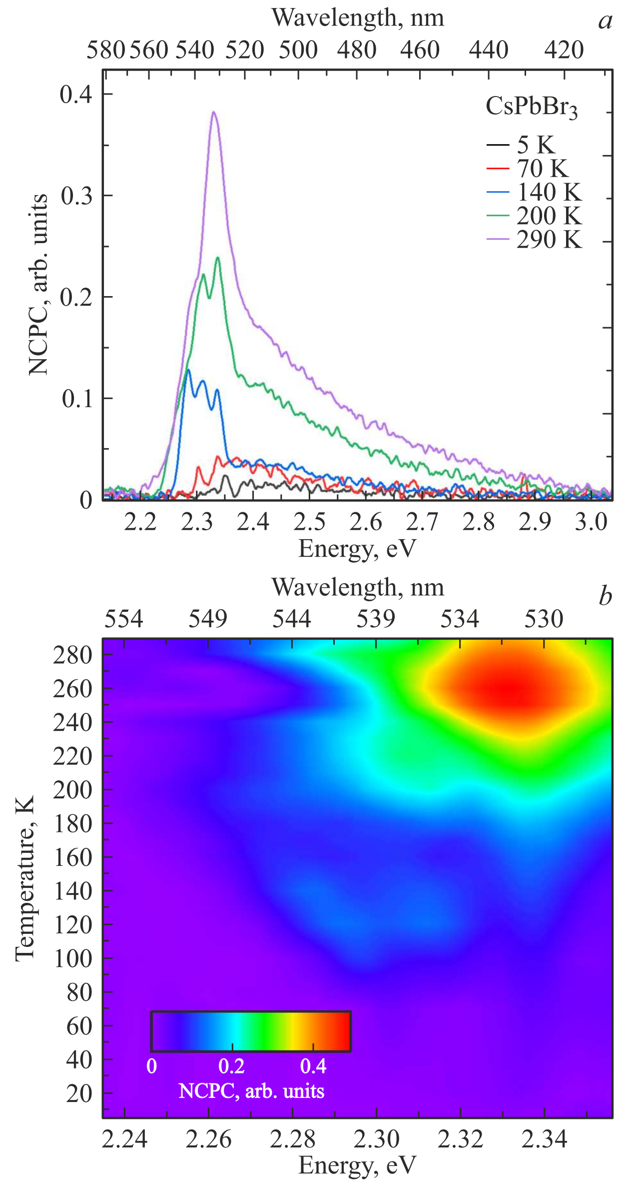

Figure 3. PC spectra of the CsPbBr$_3$ single crystal (*a*) at several temperatures, (*b*) in the form of an intensity map.

intensity above 110 K, however, as shown in Figure 2, *d*, the PL main peak positions at 320 K and 3.5 K are the same). This behavior differs from the red shift that is common to semiconductors when temperature rises and was explained by competitive impacts of thermal expansion and electron-phonon interaction [27–29].

Figure 4 shows temperature dependences of PL and PC integrated over the whole spectrum. What stands out is the fact that there is no PL when PC signal is good and, vice versa, there is no PC in the intense PL region (at low temperatures). This is because carrier freezing-out takes place as the temperature decreases, therefore, PC is reduced, however, at the same time transitions with photon emission become effective, which induces the PL signal.

Figure 5 shows the transmission, luminescence and PC spectra at 77 K in the same graph. A temperature of 77 K was chosen intentionally — PL is already observed in this range, but the PC signal hasn't disappeared yet. The 1.4 mm crystal is fully non-transparent in the exciton absorption region and upwards in energy (spectrum *1* in Figure 5). In the PL spectrum (spectrum *2* in Figure 5), a broad band that starts at the fundamental absorption edge corresponds to direct band-to-band transitions. A shortwave drop is due to the fact that, when light quantum energies are higher than the band gap, the light absorption coefficient is very high and all light is absorbed in a thin near-surface region. Two narrow intense peaks in the PC spectrum coincide in frequency with the most intense PL peaks (spectrum *3* in Figure 5) that were attributed to transitions between the localized exciton states.

Temperature dependences of the integrated high-frequency (HF) peak intensity in PL and PC assigned to

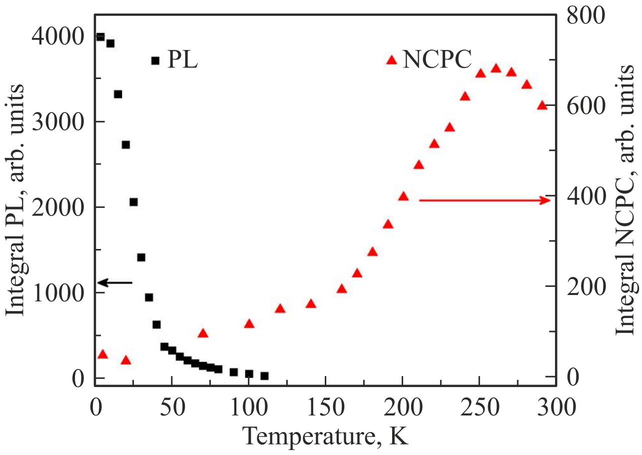

Figure 4. Temperature dependences of integrated PL (black squares) and PC (red triangles) of the CsPbBr$_3$ single crystal.

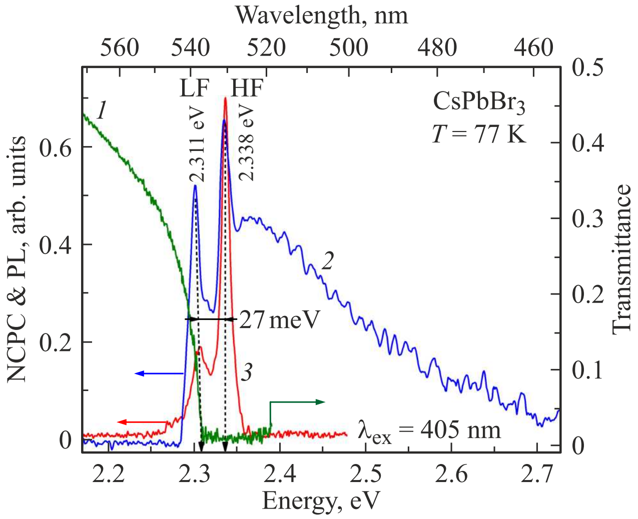

Figure 5. Transmission spectra (*1* — green), PC (*2* — blue) and PL (*3* — red) of the CsPbBr$_3$ single crystal at $T = 77$ K.

Parameters in equations (1) and (2) obtained by fitting experimental data on the temperature dependences of the HF peak in PL (in the range of 3.6–120 K) and PC (in the range of 3.6–260 K), respectively.

PL			PC				
I_0	A	E_{PL}, meV	C	B_1	$E_{(1)PC}$, meV	B_2	$E_{(2)PC}$, meV
17.9	89.4	10 ± 3	0.024	0.17	12 ± 3	11.6	77 ± 10

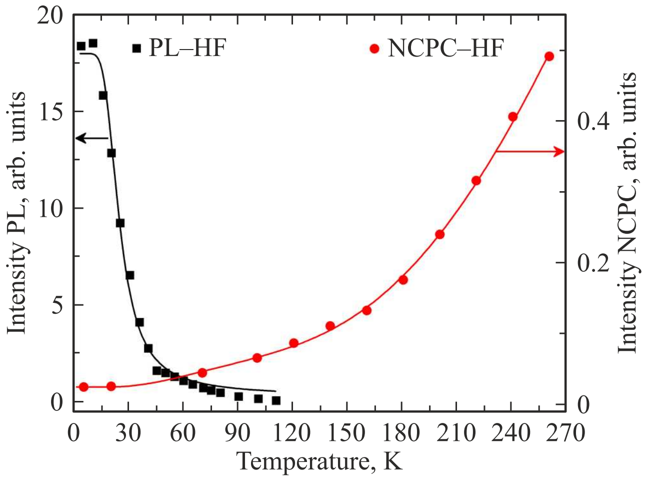

Figure 6. Temperature dependences of the integrated HF peak intensities in PL (black squares) and NCPC (red circles) of the CsPbBr$_3$ single crystal. Solid lines — approximation by equations (1) and (2) for PL and PC, respectively, with parameters from the table.

the autolocalized exciton are shown in Figure 6. Solid curves are approximations using formulas [30]

$$I_{PL}(T) = \frac{I_0}{1 + A \exp\left(\frac{E_{PL}}{kT}\right)} \tag{1}$$

and

$$I_{PC}(T) = C + B_1 \exp\left(-\frac{E_{(1)PC}}{kT}\right) + B_2 \exp\left(-\frac{E_{(2)PC}}{kT}\right) \tag{2}$$

for PL and PC, respectively (approximation parameters in formulas (1) and (2) are listed in the table). Here, k is the Boltzmann constant, E_{PL} is the energy of luminescence temperature quenching, $E_{(1)PC}$ and $E_{(2)PC}$ are the thermal activation energies of PC.

Value of E_{PL} agrees with 12 ± 3 meV obtained from the temperature dependence of luminescence intensity of the CsPbBr$_3$ nanocrystals in the region of 10–50 K [31] and is close to the difference of exciton absorption and luminescence peak energies (about 10 meV [20]). For the HF peaks of PL and PC, the activation energies E_{PL} and $E_{(1)PC}$, respectively, are close — the luminescence quenching channel coincides with the charge carrier generation channel. It may be suggested that transition of the autolocalized exciton to a free exciton is associated with an activation energy of about 10 meV. The free exciton travels along the crystal and dissociates into electron and hole — PC occurs and luminescence is quenched. PC activation energy $E_{(2)PC} = 77 \pm 10$ meV is most likely associated with direct thermal breakdown of the autolocalized exciton and creation of an electron and hole. The scope of this study doesn't include the temperature dependence of luminescence in the temperature range above 120 K, where PL is very weak. Such studies conducted in [31] gave 77 ± 18 meV for the luminescence temperature quenching energy in the range of 100–250 K [31], which agrees with the PC activation energy $E_{(2)PC} = 77 \pm 10$ meV obtained herein. Electron departure into a band from the exciton's emissive state causes PL quenching. Exciton binding energy is estimated from such interpretation of the luminescence quenching and PC activation channels: $E_b = E_{(2)PC} - E_{(1)PC} = 65 \pm 13$ meV.

Reliable data on the value of the free exciton binding energy E_b in the CsPbBr$_3$ single crystal is not available [19]. E_b is defined as the difference between the band gap width E_g and exciton peak energy position in the absorption spectrum. Experimental data for nanoparticles [32] and thin films [33] cannot be used for bulk single crystals due to considerable size effects [32–35]. Ellipsometric band gap measurements on the CsPbBr$_3$ single crystals were performed in the temperature range of 183–330 K [28]. At fixed temperature, the values of E_g differ by 40 meV depending on the data processing method [28]. There are many studies where E_b was determined by the temperature dependence of luminescence intensity [21,29,31,36,37]. The spread of results is enormous (from 37 meV [29] to 350 meV [37]) depending on the studied temperature interval and interpretation. In our opinion, such method is not adequate for determining E_b because a localized exciton luminesces rather than a free exciton.

Conclusion

This is the first study that investigates transmission spectra in the fundamental absorption edge region (1.98–2.48 eV), PL at the band-to-band excitation (405 nm) and NCPC of CsPbBr$_3$ in the temperature range of 3.6–320 K on the same single crystal. Besides the exciton peak (2.318 eV at 10 K) observed in [18,19] on perfect crystals and attributed to the autolocalized exciton luminescence, the low-temperature spectrum of the given crystal had another narrow line with a comparable intensity (2.279 eV at 10 K), additional narrow lines in the range of 2.279−2.318 eV, and a broad (73.2 meV) band with a maximum near 2.24 eV. Narrow PL lines in the range of 2.279−2.318 eV presumably refer to the exciton-impurity complexes, and the broad band may be the PL of impurity or defect centers. As the temperature increases, all lines move into the high-frequency side (which is unusual for semiconductors, but was observed in many studies concerning spectroscopy of lead-halide perovskites) and broaden, the intermediate structure disappears and two lines with comparable intensities remain above approx. 20 K.

Two narrow peaks at the intense exciton PL line frequencies and a broad band corresponding to the band-to-band absorption are observed in the PC spectrum. While PL is quenched with temperature rise, PC increases. Temperature dependences of the integrated exciton peak intensities in PC (3.6−250 K) and PL (3.6−120 K) were examined. Activation energy (10 ± 3 meV) was found for the process in the temperature range of 3.6−120 K leading to dissociation of the autolocalized exciton, PL quenching, and formation of charge carriers. This energy is presumably equal to the energy difference between the free and autolocalized exciton states. PC activation energy 77 ± 10 meV at the excitation into the exciton band of $CsPbBr_3$ in the temperature range of 100−250 K agrees with the literature data concerning PL quenching in this temperature range and is presumably equal to the distance with respect to energy from the autolocalized exciton level to the conduction band bottom. If such interpretation of the found activation energies is correct, $E_b = 65 \pm 13$ meV is obtained for the exciton binding energy in the $CsPbBr_3$ single crystal.

Acknowledgments

The authors are grateful to T.S. Sukhikh for provision of the X-ray diffraction analysis data. PL and PC spectra were measured using the unique research facility „Multifunctional high-resolution broadband spectroscopy“ (UNU MShSVR ISAN [38]).

Funding

The study was performed in the framework of state assignments of the Ministry of Science and Higher Education for the Institute of Spectroscopy, RAS № FFUU-2024-0004 (V.E.A., K.N.B.) and FFUU-2022-0003 (M.N.P.) and for Rzhanov Institute of Semiconductor Physics, Siberian Branch, RAS № FWGW-2022-0006 (O.I.S. — crystal growth).

Conflict of interest

The authors declare that they have no conflict of interest.

References

[1] S. Parola, B. Julián-López, L.D. Carlos, C. Sanchez. Adv. Funct. Mater., **26**, 6506−6544 (2016). DOI: 10.1002/adfm.201602730

[2] A.K. Jena, A. Kulkarni, T. Miyasaka. Chem. Rev., **119** (5), 3036−3103 (2019). DOI: 10.1021/acs.chemrev.8b00539

[3] S. Ullah, J. Wang, P. Yang, L. Liu, S.-E. Yang, T. Xia, H. Guo, Y. Chen. Mater. Adv., **2**, 646−683 (2021). DOI: 10.1039/d0ma00866d

[4] X. Li, Y. Wu, S. Zhang, B. Cai, Y. Gu, J. Song, H. Zeng. Adv. Funct. Mater., **26**, 2435−2445 (2016). DOI: 10.1002/adfm.201600109

[5] R. Wang, Y. Zhang, F.-X. Yu, Y. Dong, Y.-L. Jia, X.-J. Ma, Q. Xu, Y. Deng, Z.-H. Xiong, Ch.-H. Gao. J. Lumin., **219**, 116915 (2020). DOI: 10.1016/j.jlumin.2019.116915

[6] E. Oksenberg, E. Sanders, R. Popovitz-Biro, L. Houben, E. Joselevich. Nano Lett., **18** (1), 424−433 (2018). DOI: 10.1021/acs.nanolett.7b04310

[7] Z. Liu, Q. Shang, C. Li, L. Zhao, Y. Gao, Q. Li, J. Chen, S. Zhang, X. Liu, Y. Fu, Q. Zhang. Appl. Phys. Lett., **114**, 101902 (2019). DOI: 10.1063/1.5082759

[8] K.A. Drozdov, I.V. Krylov, A.S. Chizhov, M.N. Rumyantseva, L.I. Ryabova, D.R. Khokhlov. Semiconductors, **52**, 902–906 (2018). DOI: 10.1134/S1063782618070059

[9] O. Antonyak, R. Gamernyk, T. Demkiv, T. Malyi, Ya. Chornodolskyy. J. Lumin., **263**, 120030 (2023). DOI: 10.1016/j.jlumin.2023.120030

[10] B.P. Reddy, B.J. Babu, S. Sreedhar, C.K. Basha, Y. Suh, M.Ch. Sekhar, S.-H. Park. Heliyon, **10** (2), e24497 (2024). DOI: 10.1016/j.heliyon.2024.e24497

[11] B. Abasht, S.Kh. Asl, H. Aghajani, A. Asgari. Ceramics International, **50** (12), 22050−22059 (2024). DOI: 10.1016/j.ceramint.2024.03.319

[12] L. Su. J. Mat. Sci. Tech., **187**, 113−122 (2024). DOI: 10.1016/j.jmst.2024.01.003

[13] V.M. Agranovich, D.M. Basko, G.C. La Rocca, F. Bassani. J. Phys.: Condens. Matter., **10**, 9369−9400 (1998). DOI: 10.1088/0953-8984/10/42/005

[14] N. Ashurov, B.L. Oksengendler, S. Maksimov, S. Rashiodva, A.R. Ishteev, D.S. Saranin, I.N. Burmistrov, D.V. Kuznetsov, A.A. Zakhisov. Modern Electronic Mater., **3** (1), 1−25 (2017). DOI: 10.1016/j.moem.2017.05.001

[15] J. Peng, C.Q. Xia, Y.Xu, R. Li, L. Cui, J.K. Clegg, L.M. Herz, M.B. Johnston, Q. Lin. Nat. Commun., **12**, 1531 (2021). DOI: 10.1038/s41467-021-21805-0

[16] V.E. Anikeeva, K.N. Boldyrev, O.I. Semenova, T.S. Sukhikh, M.N. Popova. Opt. Mat.: X, **20**, 100259 (2023). DOI: 10.1016/j.omx.2023.100259

[17] S. Liu, A.R. DeFilippo, M. Balasubramanian, Z. Liu, S.G. Wang, Y.-S. Chen, S. Chariton, V. Prakapenka, X. Luo, L. Zhao, J.S. Martin, Y. Lin, Y. Yan, S.K. Ghose, T.A. Tyson. Adv. Sci., **8** (18), 2003046 (2021). DOI: 10.1002/advs.202003046

[18] V.V. Belykh, D.R. Yakovlev, M.M. Glazov, P.S. Grigoryev, M. Hussain, J. Rautert, D.N. Dirin, M.V. Kovalenko, M. Bayer. Nat. Commun., **10**, 673 (2019). DOI: 10.1038/s41467-019-08625-z

[19] M.P. Mamaeva, M. Androulidaki, V. Spanou, N.M. Kireev, N.T. Pelekanos, Y.V. Kapitonov, C. Stoumpos. J. Phys. Chem. C, **127** (46), 22784−22789 (2023) DOI: 10.1021/acs.jpcc.3c05829

[20] V.I. Yudin, M.S. Lozhkin, A.V. Shurukhina, A.V. Emeline, Y.V. Kapitonov. J. Phys. Chem. C, **123** (34), 21130–21134 (2019). DOI: 10.1021/acs.jpcc.9b04267

[21] Z. Zhao, M. Zhong, W. Zhou, Y. Peng, Y. Yin, D. Tang, B. Zou. J. Phys. Chem. C, **123** (41), 25349–25358 (2019). DOI: 10.1021/acs.jpcc.9b06643

[22] J.A. Steele, P. Puech, B. Monserrat, B. Wu, R.X. Yang, T. Kirchartz, H. Yuan, G. Fleury, D. Giovanni, E. Fron, M. Keshavarz, E. Debroye, G. Zhou, T.Ch. Sum, A. Walsh, J. Hofkens, M.B.J. Roeffaers. ACS Energy Lett., **4** (9), 2205–2212 (2019). DOI: 10.1021/acsenergylett.9b01427

[23] M. Isarov, L.Z. Tan, M.I. Bodnarchuk, M.V. Kovalenko, A.M. Rappe, E. Lifshitz. Nano Lett., **17** (8), 5020–5026 (2017). DOI: 10.1021/acs.nanolett.7b02248

[24] L.-I. Bulyk, T. Demkiv, O. Antonyak, Y.M. Chornodolskyy, R. Gamernyk, A. Suchocki, A. Voloshinovskii. Dalton Trans., **52**, 16712–16719 (2023). DOI: 10.1039/D3DT02647G

[25] B. Wu, H. Yuan, Q. Xu, J.A. Steele, D. Giovanni, P. Puech, J. Fu, Y.F. Ng, N.F. Jamaludin, A. Solanki, S. Mhaisalkar, N. Mathews, M.B.J. Roeffaers, M. Grátzel, J. Hofkens, T.Ch. Sum. Nat. Commun., **10**, 484 (2019). DOI: 10.1038/s41467-019-08326-7

[26] M. Dendebera, Ya. Chornodolskyy, R. Gamernyk, O. Antonyak, I. Pashuk, S. Myagkota, I. Gnilitskyi, V. Pankratov, V. Vistovskyy, V. Mykhaylyk, M. Grinberg, A. Voloshinovskii. J. Lumin., 225, 117346 (2020). DOI: 10.1016/j.jlumin.2020.117346

[27] K. Wei, Z. Xu, R. Chen, X. Zheng, X. Cheng, T. Jiang. Opt. Lett., **41** (16), 3821–3824 (2016). DOI: 10.1364/OL.41.003821

[28] G. Mannino, I. Deretzis, E. Smecca, A. La Magna, A. Alberti, D. Ceratti, D. Cahen. J. Phys. Chem. Lett., **11** (7), 2490–2496 (2020). DOI: 10.1021/acs.jpclett.0c00295

[29] Y. Yuan, M. Chen, S. Yang, X. Shen, Y. Liu, D. Cao. J. Lumin., **226**, 117471 (2020). DOI: 10.1016/j.jlumin.2020.117471

[30] D. Bimberg, M. Sondergeld, E. Grobe. Phys. Rev. B, **4**, 3451–3455 (1971). DOI: 10.1103/PhysRevB.4.3451

[31] A. Dey, P. Rathod, D. Kabra. Adv. Opt. Mater., **6**, 1800109 (2018). DOI: 10.1002/adom.201800109

[32] L. Protesescu, S. Yakunin, M.I. Bodnarchuk, F. Krieg, R. Caputo, C.H. Hendon, R.X. Yang, A. Walsh, M.V. Kovalenko. Nano Lett., **15** (6), 3692–3696 (2015). DOI: 10.1021/nl5048779

[33] C. Wolf, T.-W. Lee. Materials Today Energy, **7**, 199–207 (2018). DOI: 10.1016/j.mtener.2017.09.010

[34] J. Xu, S. Yu, X. Shang, X. Chen. Adv. Photonics Res., **4**, 2200193 (2023). DOI: 10.1002/adpr.202200193

[35] S.G. Motti, F. Krieg, A.J. Ramadan, J.B. Patel, H.J. Snaith, M.V. Kovalenko, M.B. Johnston, L.M. Herz. Adv. Funct. Mater., **30**, 1909904 (2020). DOI: 10.1002/adfm.201909904

[36] X. Shen, M. Chen, L. Shi, F. Chen, Y. Liu, D. Cao, C. Xu. Opt. Commun., **453**, 124354 (2019). DOI: 10.1016/j.optcom.2019.124354

[37] B.R.C. Vale, E. Socie, A. Burgos-Caminal, J. Bettini, M.A. Schiavon, J.-E. Moser. J. Phys. Chem. Lett., **11** (2), 387–394 (2020). DOI: 10.1021/acs.jpclett.9b03282

[38] [Electronic source]. URL:https://ckp-rf.ru/catalog/usu/508571/

Translated by E.Ilinskaya